Periodica Polytechnica Chemical Engineering, 67(1), pp. 74–82, 2023

CFD-based Estimation of Friction Factor in Rough Pipes with Herschel-Bulkley Fluids

Péter Csizmadia[1*], Gergely Dombóvári[1], Sára Till[1], Martin Minkó[2]

[1] Department of Hydrodynamic Systems, Faculty of Mechanical Engineering, Budapest University of Technology and Economics, P.O.B. 91, Budapest 1521, Hungary
[2] Wilo Hungary Ltd., Torbágy u. 22, H-2045 Törökbálint, Hungary
[*] Corresponding author, e-mail: pcsizmadia@hds.bme.hu

Received: 20 July 2022, Accepted: 06 October 2022, Published online: 09 January 2023

Abstract
The appropriate estimation of frictional losses in a pipeline system is essential. So far, little attention has been paid to determining the friction factors with non-Newtonian fluids, especially in rough pipes. This study aims at calculating the friction factor using validated three-dimensional Computational Fluid Dynamics models in Ansys CFX. Steady-state computations are performed with three different incompressible Herschel-Bulkley fluids in rough pipes with relative roughness of the inner pipe surface ε = 0.0005 – 0.01. A power-law type bath gel as a test fluid is used for experiments to validate our numerical model. The numerical results are compared with the measured values and also with numerous existing friction factor estimation models with the help of generalization of the Reynolds number in the relevant engineering range of Re_{gen} = 100 – 40,000. This paper shows that the existing approximations can not accurately describe the friction factor with pseudoplastic fluids in rough pipes. On the contrary, in the case of Bingham plastic fluid, a new, explicit calculation relation is found in a unified form accepted by the literature.

Keywords
CFD, experimental validation, friction factor, generalized Reynolds number, Herschel-Bulkley fluids, rough pipe

1 Introduction

In a pipeline system, the friction factor has a key role in hydraulic design, because knowing the losses, the systems can operate more energy-efficient. In many industrial fields, the delivered fluid has time-independent non-Newtonian rheology, e.g., the activated sludge in wastewater treatment technology [1, 2], juices [3] and pulps [4] in the food industry, the drilling mud in the oil industry [5] and chitosan ferrogel in pharmaceutical industry [6].

For Newtonian fluids, the Colebrook equation has been demonstrated applicability in the turbulent range in rough pipes and is the accepted standard of accuracy for calculated friction factors [7]. However, this equation is implicit, so it needs iteration. Therefore, numerous explicit solutions to the formula have been developed. Brkič [8] and Genić et al. [9] presented extensive reviews of the existing approaches and found many explicit approximations very accurate. Plascencia et al. [10] also compared current methods; they discovered that some expressions using Lambert's W function are also sufficiently precise. Some recent, unified formulations are valid for all hydraulic regimes for Newtonian fluids [11].

By introducing the generalized Reynolds number [12], the Darcy equation is valid for power-law, Bingham and Herschel-Bulkley laminar flows. On the contrary, there is no widely accepted model to calculate the friction factor in the turbulent regime for non-Newtonian fluids. The available equations for smooth pipes were summarized by Garcia and Steffe [13] and investigated by El-Emam et al. [14]. Turian et al. [15] experimentally investigated the friction factor with concentrated slurries, Vajargah et al. [16], Subramanian and Azar [17] with muds and Cabral et al. [18] with different liquid food products. The researchers' findings were contradictory in terms of the applicability of formulas for approximating the friction factor.

Much less is known about the friction factor with non-Newtonian fluids in rough pipes. Szilas et al. [19] and Kawase et al. [20] developed models only for power-law fluids, Reed and Pilehvari [21] and Sorgun et al. [22] for Herschel-Bulkley fluids. The latter estimations needed the wall shear stress, but no direct assessment of the wall shear stress for turbulent non-Newtonian flow is available.

Cite this article as: Csizmadia, P., Dombóvári, G., Till, S., Minkó, M. "CFD-based Estimation of Friction Factor in Rough Pipes with Herschel-Bulkley Fluids", Periodica Polytechnica Chemical Engineering, 67(1), pp. 74–82, 2023. https://doi.org/10.3311/PPch.20857

In recent years, Computational Fluid Dynamics (CFD) computations proved to be an accurate and affordable way of modelling industrial problems [23], and non-Newtonian flows [24–26]. Bartosik [27] modelled the turbulent flow of Herschel-Bulkley fluids in a smooth horizontal tube. The turbulence models for predicting flows of Herschel-Bulkley fluids were compared by Lovato et al. [28]. Singh et al. [29] conducted pipe flow simulations for Bingham and Herschel-Bulkley fluids with varying yield stress. Recently, Sorgun et al. [30] investigated the turbulent flow of viscoplastic materials in rough pipes with CFD and experiments.

The present study uses CFD to calculate the friction factor in rough pipes with different non-Newtonian fluids. Our paper provides numerical results compared to experimental ones with power-law fluids as validation. The paper also suggests parameters of a unified friction factor equation for Bingham fluids.

2 Materials and methods

2.1 Rheology

The rheological behaviour of the three investigated fluids was described with the Herschel-Bulkley (HB) model as $\tau = \tau_0 + K\dot{\gamma}^n$ where τ [Pa] is the shear stress, τ_0 [Pa] is the yield stress, K [Pas^n] is the consistency index, n [-] is the flow behaviour index and $\dot{\gamma}$[1/s] is the shear rate. The power-law (PL) and the Bingham (B) descriptions can be derived from the HB model; there is no yield stress in the PL equation, and the B model is valid when the flow behaviour index is $n = 1$.

The experimental validation was performed with a bath gel as a test fluid (Gelli Baff, compounds in [31]), a pseudoplastic material modelled with the power-law relationship. An Anton Paar Physica MCR301 rotational viscometer was used to determine the rheology. Our measurement range was 0.1–500 1/s, and the instrument was used with a cone-plate layout with a gap of 0.054 mm.

Two additional liquids from the food industry were investigated. Sani et al. [3] examined the rheology of melon juice (*Cucumis melo L. var. Inodorus*) as the function of the temperature and the total soluble solids. The properties at a temperature of 35 °C and a soluble solid 40°Brix were applied. The flow behaviour index of the pulp was nearly one, so it was considered a Bingham plastic material.

The rheology of the red guava pulp (*Psidium guajava L.*) was determined by Diniz et al. [4]. Our work used the red guava pulp at a temperature of 70 °C and a soluble solid 5.7°Brix, described with the Herschel-Bulkley model.

Table 1 Rheological parameters of the investigated fluids

Fluid	Test fluid (bath gel)	Melon juice [3] (35 °C; 40 °Brix)	Red guava pulp [4] (70 °C; 5.7 °Brix)
ρ [kg/m^3]	998	1216	963
τ_0 [Pa]	0	0.863	1.963
K [Pa·s^n]	0.150	0.075	1.311
n [-]	0.57	1	0.45
R^2	0.991	0.999	0.997
Type	PL	B	HB

Table 1 summarizes the material properties and the types of the three investigated fluids.

2.2 Friction factor formulations

The friction factor (f [-]) for rigid, straight cylindrical pipes was modelled with the Weisbach equation

$$f = \frac{\Delta p}{\frac{L}{D}\frac{\rho}{2}v^2}, \tag{1}$$

in which Δp [Pa] is the total pressure drop in the pipe section, ρ [kg/m^3] is the fluid density, L [m] is the length of the investigated section, D [m] is the inner diameter of the pipe, and v [m/s] is the mean velocity. In general, the friction factor depends on the Reynolds number Re [-] and the relative roughness of the inner pipe surface ε [-].

The Reynolds number is $\mathrm{Re} = \rho v D/\mu$ for Newtonian materials, where μ [Pas] is the dynamic viscosity of the fluid. A modified non-Newtonian Reynolds number can be written based on Metzner and Reed [32] as

$$\mathrm{Re}_{gen\_MR} = \frac{\rho v^{2-n} D^n}{K 8^{n-1}}, \tag{2}$$

but this expression does not include yield stress. Madlener et al. [12] defined another generalized Reynolds number for Herschel-Bulkley fluids:

$$\mathrm{Re}_{gen} = \frac{\rho v^{2-n} D^n}{\frac{\tau_0}{8}\left(\frac{D}{v}\right)^n + K 8^{n-1}\left(\frac{3m+1}{4m}\right)^n}, \tag{3}$$

$$m = \frac{nK\left(\frac{8v}{D}\right)^n}{\tau_0 + K\left(\frac{8v}{D}\right)^n}, \tag{4}$$

where m [-] is the local exponential factor.

In the Newtonian laminar regime, the formula for the friction factor is the theoretical Darcy equation: $f = 64/\mathrm{Re}$.

For hydraulically smooth pipes in the turbulent zone, the Blasius equation is known, where $f = 0.316/\mathrm{Re}^{0.25}$ valid for $4 \times 10^3 < \mathrm{Re} < 10^5$.

For the turbulent flows in rough pipes, the well-known implicit Colebrook equation [7] is valid for $4\times10^3 < \mathrm{Re} < 10^8$ and $0 < \varepsilon < 0.05$ as

$$\frac{1}{\sqrt{f}} = -2\log\left(\frac{\varepsilon}{3.7} + \frac{2.51}{\mathrm{Re}}\frac{1}{\sqrt{f}}\right). \tag{5}$$

The Brkič expression is based on a new approach using Lambert's W function [8]:

$$\frac{1}{\sqrt{f}} = -2\log\left(\frac{\varepsilon}{3.7} + \frac{2.18}{\mathrm{Re}}\beta\right), \tag{6}$$

where

$$\beta = \ln\left[\frac{\mathrm{Re}}{1.816\ln\left(\frac{1.1\mathrm{Re}}{1+1.1\mathrm{Re}}\right)}\right]. \tag{7}$$

Some unified friction factor formulations are valid for Newtonian fluids for all regimes from laminar to fully turbulent flow [11]. The Colebrook-Churchill formula is based on the Churchill approximation [33] of the Colebrook equation

$$f = 8\sqrt[12]{\left(\frac{8}{\mathrm{Re}}\right)^{12} + \left[\left(-2.457\ln\left(\left(\frac{7}{\mathrm{Re}}\right)^{0.9} + \frac{\varepsilon}{3.7}\right)\right)^{16} + \left(\frac{37530}{\mathrm{Re}}\right)^{16}\right]^{-1.5}} \tag{8}$$

and the Colebrook-Swamee approximation is given by Swamee and Jain [34] as

$$f = \sqrt[8]{\left(\frac{64}{\mathrm{Re}}\right)^{8} + 9.5\left[\left(\ln\left(\frac{5.74}{\mathrm{Re}^{0.9}} + \frac{\varepsilon}{3.7}\right)\right) - \left(\frac{2500}{\mathrm{Re}}\right)^{6}\right]^{-16}}, \tag{9}$$

which is closest to the conventional formulas. Furthermore, Chernikin also gave a unified equation [35]:

$$f = 0.11\sqrt[4]{\frac{\left(\frac{68}{\mathrm{Re}}\right) + \varepsilon + \left(\frac{1904}{\mathrm{Re}}\right)^{14}}{115\left(\frac{1904}{\mathrm{Re}}\right)^{10} + 1}}\,. \tag{10}$$

In this study, the Reynolds number was substituted with a generalized Re number due to Madlener et al. [12] in Eq. (3).

For non-Newtonian fluids in smooth pipes, Dodge and Metzner [36] developed the most widely used implicit expression for the Fanning friction factor f_F. For power-law fluids the Metzner-Reed Reynolds number (Eq. (2)) is used in their approach as:

$$\frac{1}{\sqrt{f_F}} = \frac{4}{n^{0.75}}\log\left(\mathrm{Re}_{gen_{MR}}\left(f_F\right)^{1-\frac{n}{2}}\right) - \frac{0.4}{n^{1.2}}\,. \tag{11}$$

The relationship between the Fanning and the Weisbach friction factors is simple: $4f_F = f$.

Only a few friction factor correlations were introduced for non-Newtonian fluids in rough pipes. The Sorgun et al. [22] model was experimentally validated with some Herschel-Bulkley fluids in the range of and and it includes the wall shear stress:

$$f_F = \frac{0.06N^{3.34}}{\left[\log\left(\frac{\varepsilon}{3.7} + 9.86\left(\mathrm{Re}_{gen_{MR}}\right)^{-N}\right)\right]^2}, \tag{12}$$

where N [-] is the function of the flow behaviour index, the yield stress and the wall shear stress $N = f(n, \tau_0, \tau_{wall})$. The Sorgun formula simplifies with PL fluids: when the flow behaviour index n can be used instead of N.

The relationship between the wall shear stress and the apparent wall shear rate ($8D/v$) for non-Newtonian fluids can be written in the following form [37]:

$$\tau_w = m'\left(\frac{8v}{D}\right)^{n'}, \tag{13}$$

where m' and n' are rheology-dependent quantities. For power-law fluids, it is known that $m' = K(3n + 1)/4n$ and $n' = n$ are constants in the laminar regime.

2.3 Simulation details

The geometry for the simulations is a straight, circular pipe section with an inner diameter of $D = 0.3$ m and $60D$ length, which is sufficiently long for a properly developed velocity profile [37]. To reduce the solver runtime, only a 9° sector of the circular cross-section was used for most simulations [24] using the symmetry boundary conditions on the edges of the geometry. This was compared with the results of the full pipe geometry with both laminar and turbulent flows. It was proved that this simplification causes at most a 0.5% difference in the calculated friction factors and at least $R^2 = 0.999$ correlation between the axial velocity profiles. The mesh of the compared full pipe and the applied 9° section are presented in Fig. 1.

A fully structured mesh of hexagonal elements was created, which consisted of 32 k elements on the reduced geometry. The grid-independence study tested twelve numerical resolutions containing approximately 12–320 k elements and proved the mesh sufficient for our task. Hence the friction factors with the selected mesh were within 0.5% of the highest resolution. Our mesh consists of 272 cells in the axial direction and 59 cells in the radial direction, including a 36-cell inflation layer near the wall. y^+ did not exceed the value of 1 in any of the smooth wall simulations; however, it increased with higher roughness values. The roughness of the pipe wall was modelled with the quantity of the sand grain roughness.

Steady-state simulations were carried out by ANSYS CFX [38], solving the continuity, the Reynold-Averaged Navier-Stokes (RANS), and the turbulent transport equations. *k–ω* Shear Stress Transport (SST) turbulence model was used with an automatic wall function setting, which is customarily considered sufficiently accurate with Herschel-Bulkley fluids [28, 39]. A uniform distribution of the mean axial velocity was specified on the inlet, and an average

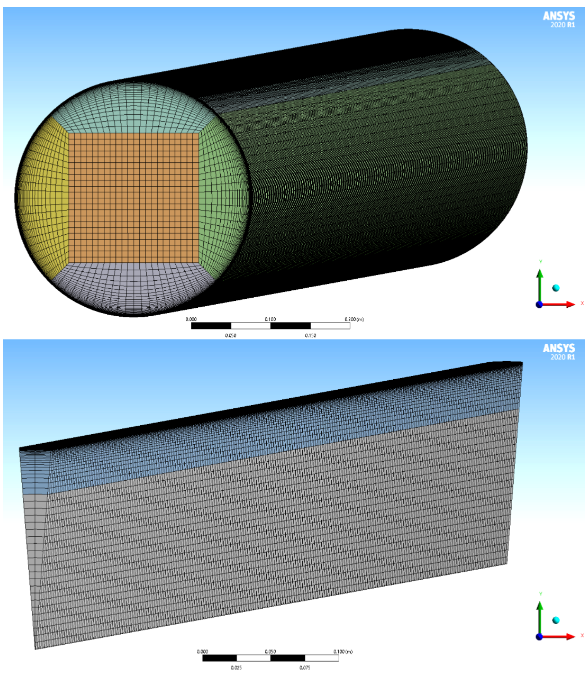

Fig. 1 The mesh of the full pipe and the 9° section

static pressure of 0 Pa on the outlet boundary. The convergence criteria varied between 10^{-5} and 10^{-6} for the Root Mean Square (RMS) values.

Wall shear stress and y^+ were evaluated before the outlet boundary. Pressure drop was calculated between two planes, 6*D* and 1*D*, from the outlet, respectively. The velocity profiles were extracted before the outlet.

2.4 Experiments

Fig. 2 presents a sketch of the experimental setup with the main elements. During the measurements, a pump (3) conveys the test fluids back to the open tank (1) via the pipeline system (2). The straight pipe section used to determine the friction factor with Eq. (1) has a 1.085 m length and an inner diameter of 0.051 m. To ensure the nearly fully developed velocity profile, the measuring section was preceded by a 0.555 m long straight pipe (at least 10*D*), similarly to [24] and [40].

The pressure drop on the straight segment of length L was measured with the help of two static pressure taps (5a) and (5b). A standard orifice meter was used to measure the volume flow rate (6), calibrated with the examined non-Newtonian fluid. All pressure drops were measured with the help of U-tube differential pressure manometers (8, 9). The accuracy of the readings was ±1 mm, and an error estimation based on this value was made at each measurement point. The volume flow rate was also checked with a Fuji Electric (FSSC1YY1) ultrasonic flowmeter (7) recommended for non-Newtonian flows.

The measuring points were set using the frequency converter mounted on the electric motor (4) and the control valve (12) on the discharge side. The fluid temperature was almost constant: 22±1 °C, so its effect on the rheological curve was neglected. The possible time-varying material structure was tested and found to be also negligible.

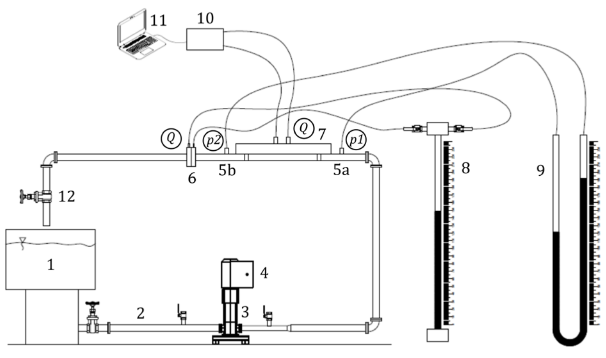

Fig. 2 The experimental setup. 1: tank, 2: pipeline system, 3: centrifugal pump, 4: electric motor, 5a, 5b: pressure taps, 6: orifice meter, 7: ultrasonic flowmeter, 8-9: U-tube manometers, 10: data acquisition device, 11: PC, 12: gate valve

3 Results

The rheological properties were used in CFD simulations to compute the friction factors. The results were compared with analytical values and the measured friction factors for smooth pipes to validate our model. Results for rough pipes were collated with the estimations detailed in Section 2.2.

3.1 Flows in smooth pipes

To validate our computations, first, the axial velocity profile was normalized with the mean velocity and presented along the dimensionless radius in Fig. 3 in laminar flow. The developed velocity profiles show the plug flow region for fluids with yield stress (B and HB fluids), which coincide with the analytically calculated dimensionless plug radius values [37], also shown in Fig. 3.

Another way to verify our numerical results is to see the wall shear stress τ_w as the function of the nominal shear rate ($8v/D$) in a smooth pipe. The bottom plot in Fig. 4 shows this relationship as representing the flow behaviour of the non-Newtonian fluids. The diagram also presents the curve fit for the three investigated fluids separately in the laminar and turbulent regimes. For our power-law test fluid in the laminar case, $m' = 0.1783$ and $n' = 0.57$ were in Eq. (12), presented with a green dotted curve (Analytical) in the figure. The numerical results matched this analytical curve with the coefficient of determination of $R^2 = 0.9884$.

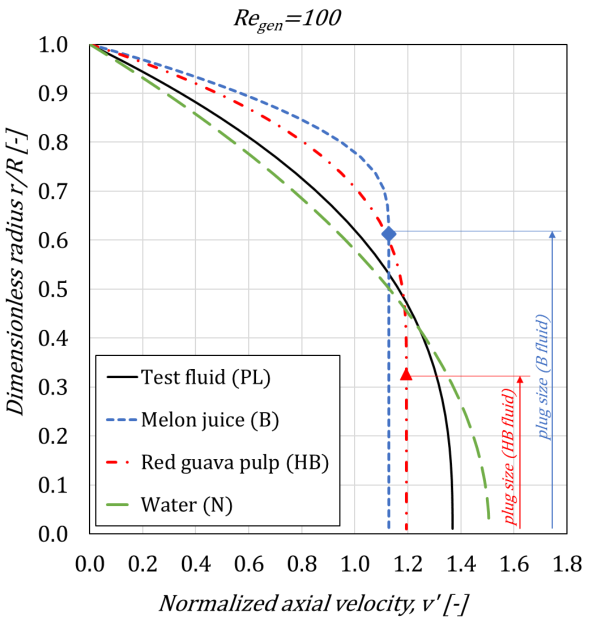

Fig. 3 Normalized axial velocity profiles in smooth pipe for the power-law, Bingham, Herschel-Bulkley fluids and with water at $Re_{gen} = 100$. Analytical dimensionless radius of the flow for the B($r_{plug,B}/R = 0.612$) and HB($r_{plug,HB}/R = 0.326$) fluids

The top panel of Fig. 4 shows the rheograms of the fluids, which confirms the crossing of the melon juice's and red guava pulp's wall shear curves. However, for the Bingham and the Herschel-Bulkley model the m' and n' parameters are considered not constants but dependent on the wall shear stress [37]; the coefficient of the determination of the fit shows that the fit assuming m' and n' constant can be acceptable approximations in these cases, too.

3.2 Validation with experiments

Since the experiments were performed in a smooth tube, the CFD results were also compared with measured and predicted friction factors with the test fluid in smooth pipe. Fig. 5 shows these friction factors of the test fluid and indicates a good agreement in the range of $100 < Re_{gen} < 8000$ with the present experiments, with the maximum difference of ±10%. The Dodge-Metzner curve was below our experimental and numerical results, as El-Emam et al. [14] and Sorgun et al. [22] also found; while our numerical results were below the Blasius equation, in which Eq. (3) was used.

The Newtonian models containing the relative roughness were very close to each other in the fully turbulent region of $4000 < Re_{gen}$. (For smooth cases, it was calculated with $\varepsilon = 0$ as suggested by the Colebrook equation.) With our PL test fluid in a smooth pipe, the Sorgun model did not prove appropriate.

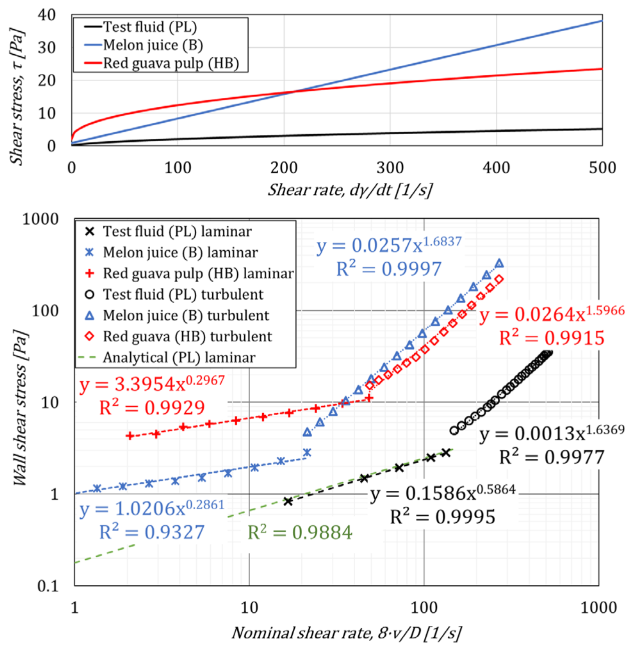

Fig. 4 Rheograms (top) and nominal shear rate-shear stress diagrams (bottom) in smooth pipe for the three investigated fluids in laminar and turbulent regimes; the analytical curve of Eq. (12) with the power-law fluid in laminar zone (green dotted)

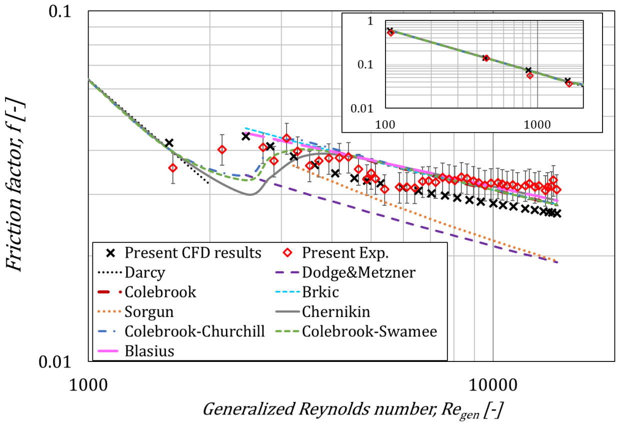

Fig. 5 Experimental (with error bar), numerical and predicted friction factors with the test fluid (PL) in smooth pipe

3.3 Results for rough pipes

The friction factors for rough pipes were compared with the formerly introduced estimation models. All the investigated approximations include the rheology using the generalized Reynolds number except for the Sorgun equation. The needed wall shear stress in the Sorgun model was estimated based on the fit presented in Fig 4. and was assessed only at $\varepsilon = 0.001$, for which value this model has been validated [22]. The numerical friction factors compared to the estimation methods are presented in Fig. 6, where (a)–(f) panels show the results in pipes with the decreasing relative roughness of ε = 0.01; 0.005; 0.002; 0.001; 0.0005 and 0 (smooth pipe). The friction factors obtained with the three type of fluids were remarkably different.

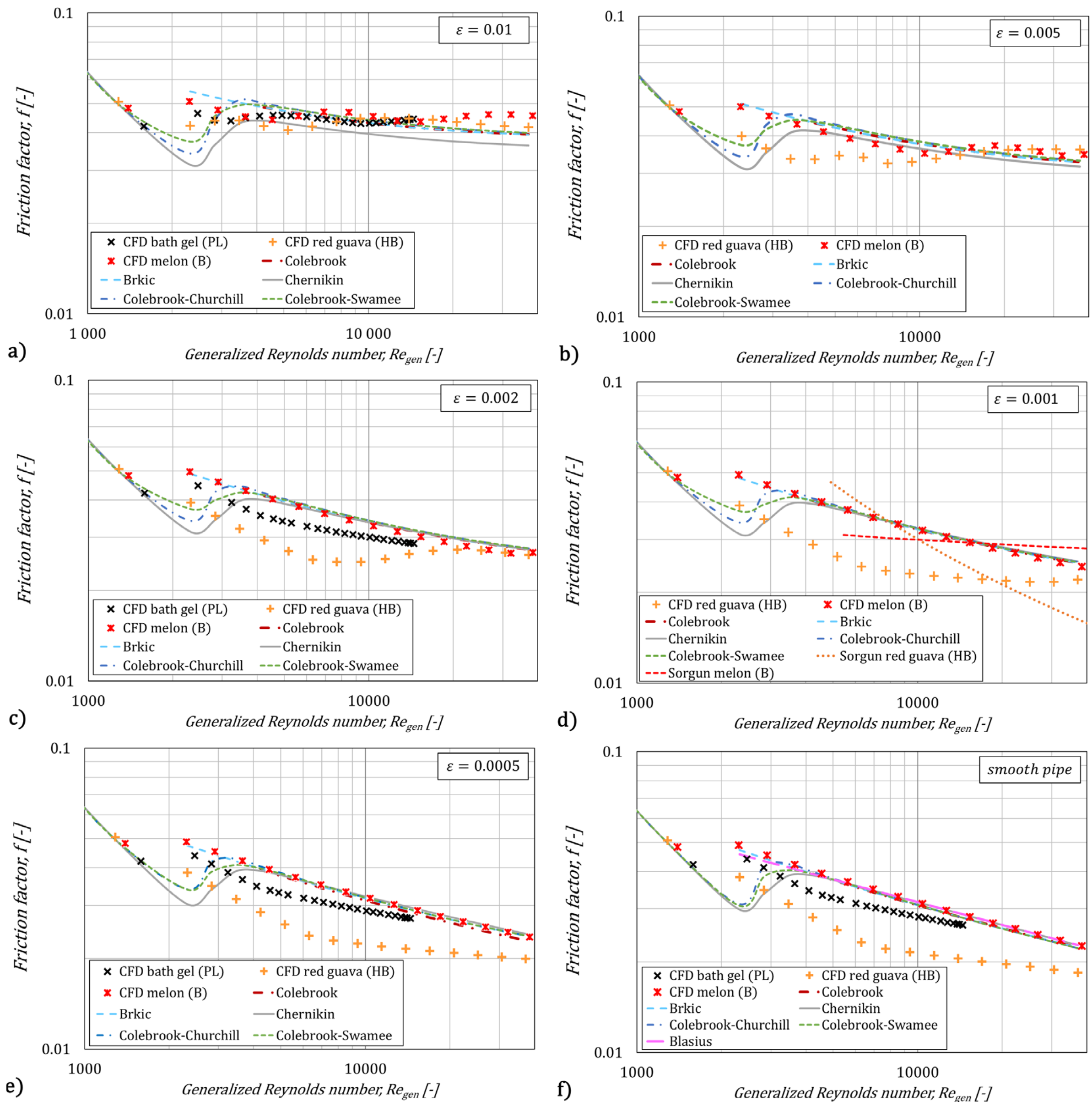

Fig. 6 Numerical and estimated friction factors with the bath gel (PL), the red guava pulp (HB) and the melon juice (B) in pipes with different roughness. a) $\varepsilon = 0.01$; b) $\varepsilon = 0.005$; c) $\varepsilon = 0.002$; d) $\varepsilon = 0.001$; e) $\varepsilon = 0.0005$; f) smooth pipe

Calculated friction factors with the Bingham type ($n = 1$) melon juice perfectly aligned with the Blasius equation in the smooth cases and with the Colebrook and Brkič predictions for all the pipes in the turbulent range. The unified approaches also seemed to be good; still, a shift in the location of the critical zone can be observed between the numerics and the estimations. Unlike the other models, the Sorgun approximation did not prove to be accurate for our Bingham fluid. The applied k–ω SST turbulence model proved to be feasible with our weakly non-Newtonian ($n \geq 0.8$ and $\tau_0/\tau_{wall} \leq 10\%$) fluid for smooth and rough pipes as well.

The best-known Colebrook-Swamee unified approximation was used to fit the Bingham results for all the investigated pipes. The exponents and the well-known parts of the equation (64/Re and ε/3.7) remained unchanged while the generalized Reynolds number in Eq. (3) was applied. So the fit extended to the parameters A, B and C in Eq. (14):

$$f = \sqrt[8]{\left(\frac{64}{\mathrm{Re}_{gen}}\right)^8 + A\left[\left(\ln\left(\frac{\boldsymbol{B}}{\mathrm{Re}_{gen}^{0.9}} + \frac{\varepsilon}{3.7}\right)\right) - \left(\frac{\boldsymbol{C}}{\mathrm{Re}_{gen}}\right)^6\right]^{-16}}, \quad (14)$$

and the curve fitting resulted in A = 12.61, B = 4.874 and C = 1375 with the goodness of fit of R^2 = 0.988 and RMSE = 0.002316 in the range of $0 \leq \varepsilon \leq 0.01$ and $260 < \mathrm{Re}_{gen} < 45000$, as seen in Fig. 7.

The other two fluids were shear-thinning; the flow behaviour index was $n = 0.57$ for PL and $n = 0.45$ for the HB fluid. As the exponent decreased, the curves moved lower in Fig. 6. However, the two liquids' flow behaviour differed also due to the Hedström number, which is an order of magnitude of 10^4 for HB and zero for the power-law fluid. These two properties together result in red guava pulp behaving quite differently from the others. Because of the pseudoplastic characteristics of these fluids, the friction factors can not be described accurately with the known estimations, interestingly including the Sorgun equation, even though it includes the wall shear stress.

Towards the zone of complete turbulence, the friction factors seemed to converge. At the highest pipe roughness, the complete turbulence occurs at lower Reynolds number values, where the friction factors agreed for all three fluids.

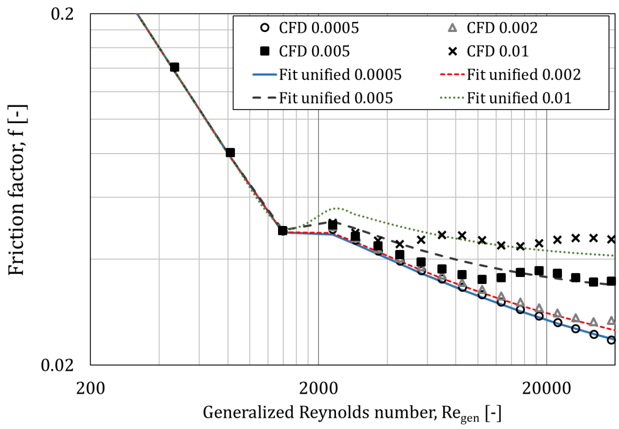

Fig. 7 Fit of the unified Colebrook-Swamee equation to the CFD results with the Bingham fluid for the rough pipes of ε = 0.01; 0.005; 0.002; 0.0005

4 Conclusions

With a validated CFD model, three-dimensional steady-state simulations were performed in Ansys CFX in a wide range of parameters on incompressible non-Newtonian fluids and achieved the following main results.

The pipe friction factor was determined for rough pipes for three Herschel-Bulkley fluids in the relevant engineering Re number and relative roughness ranges. With the generalization of the Re number, the formulas valid for the Newtonian case were extended, and thus the results were included in the literature.

For the flow of a Bingham plastic fluid in a rough pipe, a unified formula in the form accepted in the literature was defined, with which the pipe friction factor can be explicitly estimated in both laminar and turbulent regions. This result shows the applicability of the unified Colebrook-Swamee estimation for Bingham fluids.

Acknowledgements

The work was supported by the ÚNKP-21-5 New National Excellence Program of the Ministry for Innovation and Technology from the source of the National Research, Development and Innovation Fund awarded by Péter Csizmadia and the János Bolyai Research Scholarship of Hungary.

Nomenclature

A [-]	constant of the fit in Eq.(14)
B [-]	constant of the fit in Eq.(14)
C [-]	constant of the fit in Eq.(14)
D [m]	pipe inner diameter
f [-]	Weisbach friction factor
f_F [-]	Fanning friction factor

K [Pa·s^n]	consistency index
L [m]	pipe section length
m [-]	local exponential factor in Eq.(3)
m' [-]	rheology-dependent parameter in Eq.(13)
n [-]	flow behaviour index
n' [-]	rheology-dependent parameter in Eq.(13)
N [-]	flow behaviour function
p [Pa]	pressure
r_{plug} [m]	plug radius
R [m]	pipe inner radius
Re [-]	Reynolds number
Re_{gen} [-]	generalized Reynolds number
v [m/s]	mean flow velocity
β [-]	parameter in Eq.(6)
$\dot{\gamma}$ [1/s]	shear rate
ε [m]	relative roughness of the pipe
μ [Pa·s]	dynamic viscosity
ρ [kg/m^3]	density
τ [Pa]	shear stress
τ_0 [Pa]	yield stress
τ_w [Pa]	wall shear stress

Abbreviations

B	Bingham plastic fluid
CFD	Computational Fluid Dynamics
HB	Herschel-Bulkley fluid
MR	Metzner-Reed
PL	power-law fluid

References

[1] Bakos, V., Gyarmati, B., Csizmadia, P., Till, S., Vachoud, L., Göde, P. N., …, Wisniewski, C. "Viscous and filamentous bulking in activated sludge: Rheological and hydrodynamic modelling based on experimental data", Water Research, 214, 118155, 2022. https://doi.org/10.1016/j.watres.2022.118155

[2] Tóth, A. J., Gergely, F., Mizsey, P. "Physicochemical treatment of pharmaceutical process wastewater: Distillation and membrane processes", Periodica Polytechnica Chemical Engineering, 55(2), pp. 59–67, 2011. https://doi.org/10.3311/pp.ch.2011-2.03

[3] Sani, A. M., Hedayati, G., Arianfar, A. "Effect of temperature and concentration on density and rheological properties of melon (Cucumis melo L. var. Inodorus) juice", Nutrition and Food Science, 44(2), pp. 168–178, 2014. https://doi.org/10.1108/NFS-06-2013-0065

[4] Diniz, R. S., dos Reis Coimbra, J. S., Martins, M., de Oliveira dos Santos, M., Diniz, M. D. M. S., de Souza Santos, E., …, De Oliveira, E. B. "Physical properties of red guava (Psidium guajava L.) Pulp as affected by soluble solids content and temperature", International Journal of Food Engineering, 10(3), pp. 437–445, 2014. https://doi.org/10.1515/ijfe-2012-0250

[5] Kelessidis, V. C., Dalamarinis, P., Maglione, R. "Experimental study and predictions of pressure losses of fluids modeled as Herschel-Bulkley in concentric and eccentric annuli in laminar, transitional and turbulent flows", Journal of Petroleum Science and Engineering, 77(3–4), pp. 305–312, 2011. https://doi.org/10.1016/j.petrol.2011.04.004

[6] Ikhaddalene, S., Zibouche, F., Ponton, A., Irekti, A., Carn, F. "Synthesis and Rheological Properties of Magnetic Chitosan Hydrogel", Periodica Polytechnica Chemical Engineering, 65(3), pp. 378–388, 2021. https://doi.org/https://doi.org/10.3311/PPch.17148

[7] Colebrook, C. F. "Turbulent flow in pipes, with particular reference to the transition region between the smooth and rough pipe laws", Journal of the Institution of Civil Engineers, 11, pp. 133–156, 1939. https://doi.org/10.1680/ijoti.1939.13150

[8] Brkić, D. "Review of explicit approximations to the Colebrook relation for flow friction", Journal of Petroleum Science and Engineering, 77(1), pp. 34–48, 2011. https://doi.org/10.1016/j.petrol.2011.02.006

[9] Genić, S., Arandjelović, I., Kolendić, P., Jarić, M., Budimir, N., Genić, V. "A Review of Explicit Approximations of Colebrook's Equation", FME Transactions, 39, pp. 67–71, 2011.

[10] Plascencia, G., Díaz–Damacillo, L., Robles-Agudo, M. "On the estimation of the friction factor: a review of recent approaches", SN Applied Sciences, 2, 163, 2020. https://doi.org/10.1007/s42452-020-1938-6

[11] Brkić, D., Praks, P. "Unified friction formulation from laminar to fully rough turbulent flow", Applied Sciences, 8(11), 2036, 2018. https://doi.org/10.3390/app8112036

[12] Madlener, K., Frey, B., Ciezki, H. K. "Generalized Reynolds number for non-newtonian fluids", Progress in Propulsion Physics, 1, pp. 237–250, 2009. https://doi.org/10.1051/eucass/200901237

[13] Garcia, E. J., Steffe, J. F. "Comparison of Friction Factor Equations for Non-Newtonian Fluids in Pipe Flow", Journal of Food Process Engineering, 9(2), pp. 93–120, 1986. https://doi.org/10.1111/j.1745-4530.1986.tb00120.x

[14] El-Emam, N., Kamel, A. H., El-Shafei, M., El-Batrawy, A. "New equation calculates friction factor for turbulent flow of non-Newtonian fluids", Oil & Gas Journal, 101(36), pp. 74–83, 2003.

[15] Turian, R. M., Ma, T.-W., Hsu, F.-L. G., Sung, D.-J. "Flow of concentrated non-Newtonian Slurries 1: friction, losses in laminar, turbulent and transition flow through straight pipe", International Journal Multiphase Flow, 24(2), pp. 225–242, 1998.

[16] Vajargah, A. K., Sullivan, G., Johnson, M., van Oort, E. "Transitional and turbulent flow of drilling fluids in pipes: An experimental investigation", In: AADE National Technical Conference and Exhibition, Houston, TX, USA, 2017, AADE-17-NTCE-042.

[17] Subramanian, R., Azar, J. J. "Experimental study on friction pressure drop for nonnewtonian drilling fluids in pipe and annular flow", presented at: International Oil and Gas Conference and Exhibition in China, Beijing, China, Nov, 7–10, Paper Number: SPE-64647-MS, 2000.
https://doi.org/10.2118/64647-ms

[18] Cabral, R. A. F., Telis, V. R. N., Park, K. J., Telis-Romero, J. "Friction losses in valves and fittings for liquid food products", Food and Bioproducts Processing, 89(4), pp. 375–382, 2011.
https://doi.org/10.1016/j.fbp.2010.08.002

[19] Szilas, A. P., Bobok, E., Navratil, L. "Determination of turbulent pressure loss of non-newtonian oil flow in rough pipes", Rheologica Acta, 20(5), pp. 487–496, 1981.
https://doi.org/10.1007/BF01503271

[20] Kawase, Y., Shenoy, A. V., Wakabayashi, K. "Friction and heat and mass transfer for turbulent pseudoplastic non-newtonian fluid flows in rough pipes", The Canadian Journal of Chemical Engineering, 72(5), pp. 798–804, 1994.
https://doi.org/10.1002/cjce.5450720505

[21] Reed, T. D., Pilehvari, A. A. "New model for laminar, transitional, and turbulent flow of drilling muds", In: SPE Production Operations Symposium, Oklahoma City, OK, USA, 1993, pp. 469–482. ISBN: 978-1-55563-490-2
https://doi.org/10.2523/25456-ms

[22] Sorgun, M., Muftuoglu, T. D., Gucuyener, I. H. "Friction factor estimation for turbulent flow of Herschel-Bulkley and power law fluids in pipes", Journal of Petroleum Science and Engineering, 211, 110044, 2021.
https://doi.org/10.1016/j.petrol.2021.110044

[23] Sass, Á., Kummer, A., Ulbert, Z., Egedy, A. "Failure Analysis of Heat Exchangers with a Valid CFD Simulation", Periodica Polytechnica Chemical Engineering, 65(4), pp. 536–549, 2021.
https://doi.org/https://doi.org/10.3311/PPch.17095

[24] Csizmadia, P., Hős, C. "CFD-based estimation and experiments on the loss coefficient for Bingham and power-law fluids through diffusers and elbows", Computers and Fluids, 99, pp. 116–123, 2014.
https://doi.org/10.1016/j.compfluid.2014.04.004

[25] Valdés, J. P., Becerra, D., Rozo, D., Cediel, A., Torres, F., Asuaje, M., Ratkovich, N. "Comparative analysis of an electrical submersible pump's performance handling viscous Newtonian and non-Newtonian fluids through experimental and CFD approaches", Journal of Petroleum Science and Engineering, 187, 106749, 2020.
https://doi.org/10.1016/j.petrol.2019.106749

[26] Bíbok, M., Csizmadia, P., Till, S. "Experimental and Numerical Investigation of the Loss Coefficient of a 90° Pipe Bend for Power-Law Fluid", Periodica Polytechnica Chemical Engineering, 64(4), pp. 469–478, 2020.
https://doi.org/10.3311/ppch.14346

[27] Bartosik, A. "Modelling of a turbulent flow using the Herschel-Bulkley rheological model", Chemical and Process Engineering, 27, pp. 623–632, 2006.

[28] Lovato, S., Keetels, G. H., Toxopeus, S. L., Settels, J. W. "An eddy-viscosity model for turbulent flows of Herschel–Bulkley fluids", Journal of Non-Newtonian Fluid Mechanics, 301, 104729, 2022.
https://doi.org/10.1016/j.jnnfm.2021.104729

[29] Singh, J., Rudman, M., Blackburn, H. M. "The effect of yield stress on pipe flow turbulence for generalized newtonian fluids", Journal of Non-Newtonian Fluid Mechanics, 249, pp. 53–62, 2017.
https://doi.org/10.1016/j.jnnfm.2017.09.007

[30] Sorgun, M., Ulker, E., Uysal, S. O. K., Muftuoglu, T. D. "CFD modeling of turbulent flow for Non-Newtonian fluids in rough pipes", Ocean Engineering, 247, 110777, 2022.
https://doi.org/10.1016/j.oceaneng.2022.110777

[31] Fry, L. "A Toxicological Risk Assessment (TRA) for Gelli Baff", Exponent Inc., Alexandria, VA, USA, Rep. 1108587.001 BF00 0712 RR01, 2011.

[32] Metzner, A. B., Reed, J. C. "Flow of Non-Newtonian Fluids-Correlation of the Laminar, Transition, and Turbulent-flow Regions", American Institute of Chemical Engineers Journal, 1(4), pp. 434–440, 1955.
https://doi.org/10.1002/aic.690010409

[33] Churchill, S. W. "Empirical expressions for the shear stress in turbulent flow in commercial pipe", American Institute of Chemical Engineers Journal, 19(2), pp. 375–376, 1973.
https://doi.org/10.1002/aic.690190228

[34] Swamee, P. K., Jain, A. K. "Explicit Equations for Pipe-Flow Problems", Journal of the Hydraulics Division, 102(5), pp. 657–664, 1976.
https://doi.org/10.1061/JYCEAJ.0004542

[35] Chernikin, A. V., Chernikin, V. A. "Обобщенная Формула Для Расчета Коэффициента Гидравлического Сопротивления Магистральных Трубопроводов Для Светлых Нефтепродуктов И Маловязких Нефтей" (Unified Formula for Calculation of Hydraulic Resistance Coefficient in Pipelines For Light Oil Products and Low Viscosity Oils), Science & Technologies: Oil and Oil Products Pipeline Transportation, 4(8), pp. 4–6, 2012. (in Russian)

[36] Dodge, D. W., Metzner, A. B. "Turbulent Flow of Non-Newtonian Systems", American Institute of Chemical Engineers Journal, 5(2), pp. 189–204, 1959.
https://doi.org/10.1002/aic.690050214

[37] Chhabra, R. P.; Richardson, J. F. "Non-Newtonian Flow and Applied Rheology: Engineering Applications", 2nd ed., Butterworth-Heinemann, 2008. ISBN 978-0-7506-8532-0
https://doi.org/10.1016/B978-0-7506-8532-0.X0001-7

[38] ANSYS "Chapter 1. Basic Solver Capability Theory and Chapter 2. Turbulence and Wall Function Theory", In: ANSYS CFX Solver Theory Guide, Canonsburg, PA, USA, 2009, pp. 1-97.

[39] Csizmadia, P., Till, S. "The effect of rheology model of an activated sludge on to the predicted losses by an elbow", Periodica Polytechnica Mechanical Engineering, 62(4), pp. 305-311, 2018.
https://doi.org/10.3311/PPme.12348

[40] Kfuri, S. L. D., Silva, J. Q., Soares, E. J., Thompson, R. L. "Friction losses for power-law and viscoplastic materials in an entrance of a tube and an abrupt contraction", Journal of Petroleum Science and Engineering, 76(3–4), pp. 224–235, 2011.
https://doi.org/10.1016/j.petrol.2011.01.002